Structural, Magnetic and Electronic Properties of (110)-Oriented Epitaxial Thin Films of the Bilayer Manganite $La_{1.2}Sr_{1.8}Mn_2O_7$

Yayoi Takamura, Jostein K. Grepstad,[a] Rajesh V. Chopdekar,[b] and Yuri Suzuki

Department of Materials Science and Engineering, University of California, Berkeley and Lawrence Berkeley National Laboratory, Berkeley, CA, USA, 94720

Ann F. Marshall,

Laboratory for Advanced Materials, Stanford University, Stanford, CA, USA, 94305

Hong Zheng and John F. Mitchell

Materials Science Division, Argonne National Laboratory, Argonne, IL, USA, 60439

We have synthesized (110)-oriented epitaxial thin films of the bilayer (n=2) manganite, $La_{1.2}Sr_{1.8}Mn_2O_7$, with the metallic/ferromagnetic *a*-*b* planes lying perpendicular to the substrate surface and the *c*-axis aligned in the plane of the film. X-ray diffraction and transmission electron microscopy confirm the alignment of the *a*-*b* planes along the $[1\bar{1}0]$ substrate direction. The films consist primarily of the n=2 phase with a minor component of the n=1 $(La,Sr)_2MnO_4$ and n=∞ $(La,Sr)MnO_3$ phases. A resistivity maximum coincides with a ferromagnet/paramagnet transition at a reduced T_c~90K (vs. 120K for bulk), indicative of the effects of epitaxial strain. The films display similar anisotropic properties to their bulk counterpart with the magnetically easy direction confined to the *a*-*b* planes and 20–200 times lower resistivity for current flowing along the *a*-*b* planes compared to the *c*-axis.

---

[a] Also affiliated with Norwegian University of Science and Technology, Trondheim, NORWAY

[b] Also affiliated with School of Applied and Engineering Physics, Cornell University, Ithaca, NY, 14853

Complex oxide materials exhibit a wide range of technologically relevant properties, including novel magnetic, electronic and optical properties. In particular, the quasi-two dimensional (2D) bilayer manganites form model systems for the study of magnetism at reduced dimensions. These materials belong to the Ruddlesden-Popper (RP) family, which can be represented as $AO\cdot(R_{1-x}A_xMnO_3)_n$ for the doped rare-earth manganites, where R=trivalent rare-earth lanthanide, A=divalent alkaline earth, n=number of perovskite layers per block, and x=doping level. This naturally layered material consists of interleaved blocks of n metallic/ferromagnetic (M/FM) layers with the perovskite $R_{1-x}A_xMnO_3$ structure and an insulating AO rocksalt layer. The amount of coupling between the M/FM layers depends on n, ranging from a 2D system for small n to a 3D system as n approaches ∞. Therefore, this class of layered materials enables us to study the properties of ultrathin M/FM layers as well as the electronic and magnetic coupling among such layers.

Much of the work on the layered RP manganites has focused on bulk crystals of the n=2 version of the Sr-doped lanthanum manganite, $La_{2-2x}Sr_{1+2x}Mn_2O_7$,[1-3] whose magnetic structure depends strongly on the doping level. Recently, Freeland *et al.*[4] have shown that as a result of the 2D nature of this system, the magnetic dead layer, which extends to a depth of 5 nm in the n=∞ perovskite $La_{0.7}Sr_{0.3}MnO_3$,[5] remains confined to the topmost bilayer (~1 nm) while the next bilayer possesses the full spin polarization of the bulk. Therefore, by depositing a ferromagnetic top electrode, an ideal magnetic tunnel junction could be created with the "nanoskin" serving as an intrinsic and uniform insulating tunnel barrier.[4]

Previous thin film reports have been mostly limited to c-axis oriented films grown on (001)-oriented $SrTiO_3$ (STO) substrates with the $La_{1-x}Sr_xMnO_3$ bilayers (a-b planes)

parallel to the substrate surface. Konishi *et al.*[6] found that their films exhibited coincident ferromagnetic/paramagnetic (FM/PM) and metal/insulator (M/I) transitions that were broadened and shifted to lower temperatures by ~20 K compared to the bulk. Philipp *et al.*[7] measured both the resistivity parallel to the *c*-axis, r_c, and parallel to the *a*-*b* planes, r_{ab}, using a mesa structure and reported an anisotropy ratio, r_c/r_{ab}~1000 for all temperatures, compared to bulk values of r_c/r_{ab}~100-200.[1,8,9] Meanwhile, only a single group has reported *a*-axis oriented films for *n*=2 Ca-doped RP manganites with twin domains that make their resistivity data consist of a superposition of r_c and r_{ab} components.[10]

In this letter, we present the synthesis and characterization of (110)-oriented epitaxial $La_{1.2}Sr_{1.8}Mn_2O_7$ (x=0.4, n=2) thin films where the $La_{1-x}Sr_xMnO_3$ layers are oriented perpendicular to the substrate surface. This particular orientation enables us to probe the magnetic and transport anisotropy of this quasi-2D bilayer manganite in the same sample. The films display anisotropic magnetic and electronic properties with the magnetically easy direction parallel to the *a*-*b* planes and an anisotropy field greater than 3 T along the magnetically hard direction. Using patterned bars, an anisotropy ratio, r_c/r_{ab}~20–200 was measured over the temperature range from 5–380 K. The FM/PM transition at T_c~90 K (vs. 120 K in bulk) coincides with a resistivity maximum and the low temperature magnetic phase is characterized by a magnetoresistance near -100%.

The (110)-oriented films of $La_{1.2}Sr_{1.8}Mn_2O_7$ were grown by pulsed laser deposition with thicknesses ranging from 100 to 600 nm. The KrF excimer laser (248 nm) was operated at 10 Hz and a fluence of 1.4 J/cm^2, while the substrate temperature was held at 900°C and the oxygen pressure was 100 mTorr. The choice of (110)-orientated STO substrates allows us to control the orientation of the $La_{1-x}Sr_xMnO_3$

bilayers such that they lie perpendicular to the substrate plane with the *c*-axis (20.14 Å) in the plane of the film along the $[001]$ substrate direction. The short *a*-axis ($a = b = 3.87$ Å) lies at an angle of 45° relative to the sample surface as shown in Fig. 1a. The films experience a tensile strain of 0.9% along the $[1\bar{1}0]$ direction and a large compressive strain of 3.2% along the $[001]$ direction.

Atomic force microscopy images (AFM) of the (110)-oriented $La_{1.2}Sr_{1.8}Mn_2O_7$ films (Fig. 1b) reveal a characteristic morphology of rectangular grains with their long axis oriented with the $[1\bar{1}0]$ substrate direction. The elongation along the $[1\bar{1}0]$ direction indicates that the fast growth direction is along the *a*-*b* planes, in agreement with reports for bulk crystal growth.[11] Rutherford backscattering spectroscopy confirms the stoichiometry of the films to within the 5% compositional accuracy of this technique. The x-ray diffraction (XRD) q-$2q$ scans display only (*hh*0) film peaks on the high angle side of the (*hh*0) substrate peaks, indicating the presence of only (110)-oriented grains. Since all members of the RP family share nearly the same *a*-axis lattice constant, these peaks could be equally likely due to any phase in the series. The identity of the phases and their orientation with respect to the substrate were confirmed using pole figures taken around the (116) film peak for the n=2 phase and the (112) film peak for the n=1 phase. These pole figures indicate that the predominant phase is the n=2 phase, though a minor component of the n=1 phase exists as well. The two-fold symmetry of both pole figures confirms that the *a*-*b* planes are oriented along the $[1\bar{1}0]$ substrate direction for both phases. The presence of the n=1 phase is not completely unexpected as previous work on bulk samples reported that other phases can amount to between 1 to 10% of the sample by mass.[12,13] However, this phase possesses a substantial *c*-axis lattice mismatch (6.7%

compressive) with the underlying STO substrate and it has been shown to be neither ferromagnetic nor metallic in bulk form.[1,14] Furthermore, in order to maintain the overall stoichiometry of the film, there must exist an equal amount of n=1 and n=∞ phases.

Low-resolution plan-view TEM images show that the rectangular grains observed in the AFM images are crystalline and partially separated in the [001] direction by 60-100 Å wide amorphous regions. Because these amorphous regions are limited in length (less than 200 nm), they are not believed to significantly affect either the magnetic or transport properties of the films. A typical high-resolution image of the 600 nm thick film (Fig. 1c) shows that the layering of SrO and $La_{1-x}Sr_xMnO_3$ planes along the c-axis is comprised predominantly (~70%) of the n=2 phase, with a 10.2 Å spacing (c/2).[1,11,12] Interspersed are individual layers and small extended slabs of the n=1 phase (c/2=6.2 Å).[14] The arrow at the bottom of the figure highlights a series of antiphase boundaries where the layering changes along the $[1\bar{1}0]$ direction. As the thickness of the film decreases, the proportion of the n=1 phase observed in the TEM images increases. The diffraction pattern (inset in Fig. 1c) reflects the layering disorder along the c-axis. While the horizontal spacing corresponds to the expected $(1\bar{1}0)$ plane spacing (2.74 Å) for the $La_{1.2}Sr_{1.8}Mn_2O_7$ phase, the vertical (c-axis) spots are streaked and incommensurately spaced. The incommensurate five-fold spacing between the direct beam (DB) and the first basic spot, (corresponding to the basic cubic perovskite lattice), represents the layering disorder with the n=2 phase dominating. For thinner films, an incommensurate three-fold spacing indicates the higher volume fraction of the n=1 phase. These results indicate that the interface layer consists of a mixture of the n=1, n=2, and n=∞ phases, while the topmost portion of the film consists primarily of the n=2 phase. Overall, the films consist of

rectangular, crystalline grains decorated by antiphase boundaries and partially separated by amorphous regions.

Magnetization measurements of the $La_{1.2}Sr_{1.8}Mn_2O_7$ films (Fig. 2) were performed in a SQUID magnetometer with two in-plane field (H_a) orientations, H_a // *c*-axis (open symbols) and H_a // *a*-*b* planes (closed symbols). A large uniaxial anisotropy in the magnetic behavior can be observed for both the magnetization as a function of temperature (Fig. 2a) and as a function of applied field (Fig. 2b). In agreement with previous single crystal results,[1,3,9,11,15] the easy direction lies parallel to the *a*-*b* planes, with an associated anisotropy field in excess of 3 T.

The magnetization vs. temperature graph shown in Fig. 2a demonstrates that the majority phase consists of $La_{1.2}Sr_{1.8}Mn_2O_7$ with a T_c~90 K. This value is suppressed and broadened compared to the bulk value of 120 K, shown as the solid line, in agreement with previous thin film results with the *c*-axis out-of-plane geometry.[6,7] Neutron powder diffraction on bulk samples showed that the magnetic transition at 120 K is accompanied by a sharp increase in the *c* lattice parameter and a decrease in the *a* lattice parameter.[12] Because the thin film is clamped to the substrate, this change in structure leads to increased strain in both in-plane directions, and likely causes the observed suppression and broadening of the magnetic transition. Two weaker magnetic transitions occur at 225 K and 360 K for thin films and target material alike. The transition at 360 K indicates the presence of the $n=\infty$ $La_{1-x}Sr_xMnO_3$ phase with $0.25<x<0.6$,[16] which is expected to accompany the $n=1$ phase observed in the XRD data and TEM images. While the exact origin of the magnetic transition at 225 K remains unclear, it can possibly be attributed to the $n=\infty$ phase with x~0.15[16] or to intergrowths with $n\neq2$ which have been shown to result in a magnetic transition around 250-300 K in bulk single crystal samples.[9,13,15,17] As

the film thickness increases from 100 to 600 nm, the proportion of the high T_c phases remains constant while the amount of $La_{1.2}Sr_{1.8}Mn_2O_7$ increases. This lack of magnetism in the thinner films supports the TEM analysis that the non-magnetic *n*=1 phase resides primarily at the substrate/film interface, while the topmost portion of the film consists mainly of the ferromagnetic *n*=2 phase.

Magnetotransport measurements of the anisotropic resistivity components r_c and r_{ab} were performed by patterning bars 250 μm wide and 2 mm long along the $[001]$ and $[1\bar{1}0]$ directions, respectively, on the same substrate. Fig. 3 plots r_{ab} (closed symbols) and r_c (open symbols) as a function of temperature for H_a // *a-b* planes for a 300 nm thick film at 0.0, 2.5, and 5.0 T. Both r_{ab} and r_c decrease with increasing magnetic field at low temperatures, indicative of the suppression of spin fluctuations. In addition, both curves exhibit similar temperature dependences with an anisotropy ratio, r_c/r_{ab}~20–200 over the temperature range studied (5–380 K). While the 300 nm thick film shows a resistivity maximum at ~90 K, thinner films (~100 nm) exhibit insulating behavior, i.e. increasing resistivity with decreasing temperature, which is expected for the *n*=1 phase. A clear M/I transition is not observed in the 300 nm thick film due to the presence of interspersed regions of the *n*=1 and *n*=∞ phases in the film. The low temperature magnetoresistance, $MR = \frac{[r(H) - r(H=0)]}{r(H=0)} \times 100$ for the $La_{1.2}Sr_{1.8}Mn_2O_7$ phase reaches a value near -100% at 5 T.

In conclusion, we have grown (110)-oriented epitaxial thin films of the $La_{1.2}Sr_{1.8}Mn_2O_7$ bilayer manganite on (110)-oriented STO substrates. The films display anisotropic magnetic and electronic properties with the magnetically easy direction parallel to the *a-b* planes and an anisotropy ratio, r_c/r_{ab}~20–200 over the temperature

range from 5–380 K. A resistivity maximum coincides with a FM/PM transitions at T_c~90 K (vs. 120 K in bulk), below which the *MR* reaches -100% at 5T.

This work was funded by the U.S. Department of Energy, Basic Energy Sciences, under Contract No.s DE-AC02-05CH11231 and W-31-109-ENG-38, through the Center for Excellence in Synthesis and Processing of Spintronic Oxides. We thank K.M. Yu for the RBS measurements and M. Weathers for the pole figure analysis.

Figure Captions

FIG. 1: (a) Schematic showing the orientation of the $La_{1.2}Sr_{1.8}Mn_2O_7$ films grown on (110)-oriented STO substrate. (b) AFM image showing the rectangular morphology of the films with the long axis along the $[1\bar{1}0]$ direction. (c) High-resolution plan-view TEM image of a 600 nm thick film indicating the presence of two predominant spacings, 6.2 Å and 10.1 Å, corresponding to the *n*=1 and *n*=2 phases of the RP series, respectively. Diffraction pattern is included as inset.

FIG. 2: Magnetization (a) as a function of temperature at 500 Oe and (b) as a function applied field at 5 K for H_a // *a*-*b* planes (closed symbols) and H_a // *c*-axis (open symbols) for a 600 nm thick film. Data for the target material is shown as a solid line.

FIG. 3: r_{ab} (closed symbols) and r_c (open symbols) as a function of temperature for a 300 nm thick $La_{1.2}Sr_{1.8}Mn_2O_7$ film with H_a // *a*-*b* planes at 0.0, 2.5 and 5.0 T.

References

[1] Y. Moritomo, A. Asamitsu, H. Kuwahara, and Y. Tokura, *Nature* **380,** 141 (1996).

[2] T. Kimura, Y. Tomioka, H. Kuwahara, A. Asamitsu, M. Tamura, and Y. Tokura, *Science* **274,** 1698 (1996).

[3] J. F. Mitchell, D. N. Argyriou, A. Berger, K. E. Gray, R. Osborn, and U. Welp, *J. Phys. Chem. B* **105,** 10731 (2001).

[4] J. W. Freeland, K. E. Gray, L. Ozyuzer, P. Berghuis, E. Badica, J. Kavich, H. Zheng, and J. F. Mitchell, *Nat. Mater.* **4,** 62 (2005).

[5] See for example J.H. Park, H.J. Kim, C. Kwon, R. Ramesh, and T. Venkatsen, *Phys. Rev. Lett*. **81**, 1953 (1998) and J.Z. Sun, D.W. Abraham, R.A. Rao, and C.B. Eom, *Appl. Phys. Lett*. **74**, 3017 (1999).

[6] Y. Konishi, T. Kimura, M. Izumi, M. Kawasaki, and Y. Tokura, *Appl. Phys. Lett.* **73,** 3004 (1998).

[7] J. B. Philipp, J. Klein, C. Recher, T. Walther, W. Mader, M. Schmid, R. Suryanarayanan, L. Alff, and R. Gross, *Phys. Rev. B* **65,** 184411 (2002).

[8] Q. A. Li, K. E. Gray, and J. F. Mitchell, *Phys. Rev. B* **63,** 024417 (2000).

[9] C. L. Zhang, X. J. Chen, C. C. Almasan, J. S. Gardner, and J. L. Sarrao, *Phys. Rev. B* **65,** 134439 (2002).

[10] H. Asano, J. Hayakawa, and M. Matsui, *Phys. Rev. B* **56,** 5395 (1997).

[11] K. Hirota, Y. Moritomo, H. Fujioka, M. Kubota, H. Yoshizawa, and Y. Endoh, *J. Phys. Soc. Jpn.* **67,** 3380 (1998).

[12] J. F. Mitchell, D. N. Argyriou, J. D. Jorgensen, D. G. Hinks, C. D. Potter, and S. D. Bader, *Phys. Rev. B* **55,** 63 (1997).

[13] C. D. Potter, M. Swiatek, S. D. Bader, D. N. Argyriou, J. F. Mitchell, D. J. Miller, D. G. Hinks, and J. D. Jorgensen, *Phys. Rev. B* **57,** 72 (1998).

[14] Y. Moritomo, Y. Tomioka, A. Asamitsu, Y. Tokura, and Y. Matsui, *Phys. Rev. B* **51,** 3297 (1995).

[15] S. D. Bader, R. M. Osgood, D. J. Miller, J. F. Mitchell, and J. S. Jiang, *J. Appl. Phys.* **83,** 6385 (1998).

[16] A. Urushibara, Y. Moritomo, T. Arima, A. Asamitsu, G. Kido, and Y. Tokura, *Phys. Rev. B* **51,** 14103 (1995).

[17] R. Seshadri, M. Hervieu, C. Martin, A. Maignan, B. Domenges, B. Raveau, and A. N. Fitch, *Chem. Mater.* **9,** 1778 (1997).

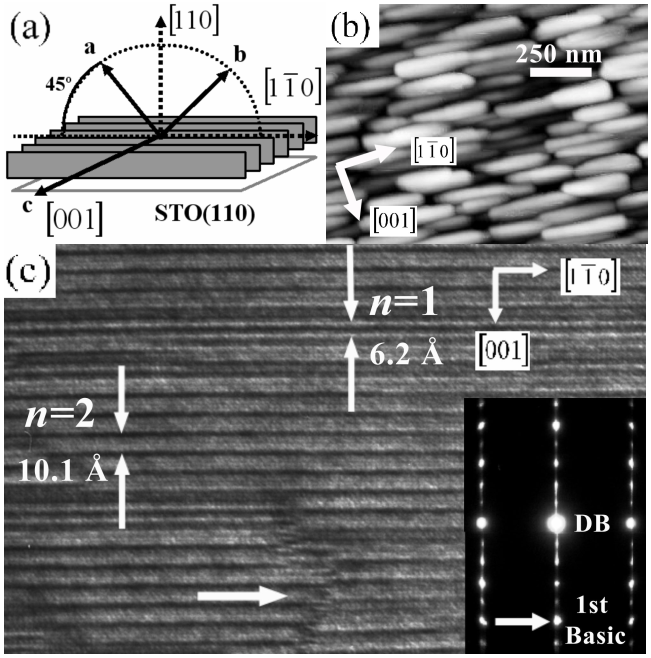
(a)
[110]
a
b
45°
[1 1̄ 0]
c
[001]
STO(110)
(b)
250 nm
[1 1̄ 0]
[001]
(c)
n=1
6.2 Å
[1 1̄ 0]
[001]
n=2
10.1 Å
DB
1st
Basic

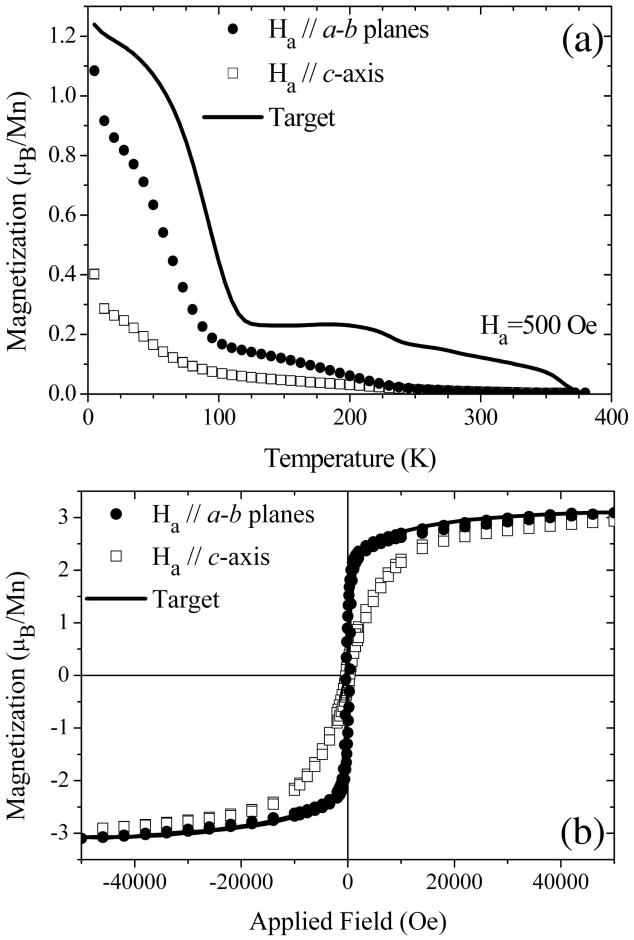
(a)
H_a // a-b planes
H_a // c-axis
Target
H_a=500 Oe
Magnetization (μ_B/Mn)
Temperature (K)
(b)
H_a // a-b planes
H_a // c-axis
Target
Magnetization (μ_B/Mn)
Applied Field (Oe)

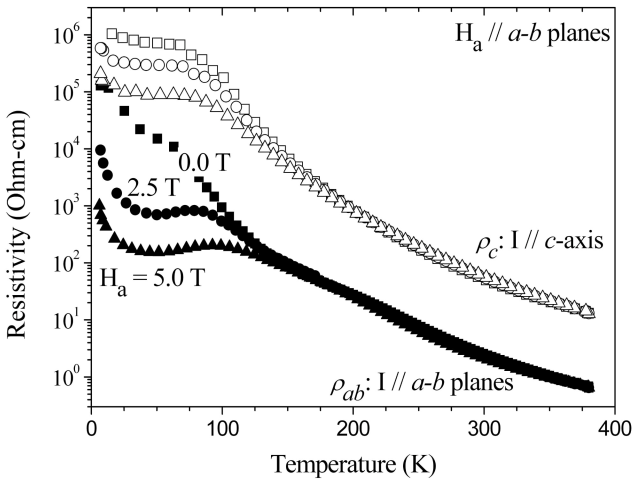
Resistivity (Ohm-cm)
Temperature (K)
H_a // a-b planes
0.0 T
2.5 T
H_a = 5.0 T
ρ_c: I // c-axis
ρ_ab: I // a-b planes